GMR
The Original

ANTIMICROBIAL POTENTIAL OF GREEN SYNTHESIZED CuO NANOPARTICLES LOADED POLYMERIC ELECTROSPUN NANOSCAFFOLDS FROM *Sargassum wightii* EXTRACT

Karneesh Kumar[1], Nandha Kumar S[2], Sattanathan Govindharajan[3]*

[1]Saveetha Medical College & Hospital (SMCH), Saveetha Institute of Medical and Technical Sciences (SIMATS), Thandalam, Chennai, Tamil Nadu 602105, India. kkarneesh8@gmail.com
[2]Department of Cardiology, Saveetha Medical College and Hospital, Saveetha Institute of Medical And Technical Sciences (SIMATS), Thandalam, Chennai-602105, Tamil Nadu, India. Email: drnandhakumar1@gmail.com
[3]Department of Pathology, Saveetha Medical College and Hospital, Saveetha Institute of Medical And Technical Sciences (SIMATS), Thandalam, Chennai-602105, Tamil Nadu, India. Email: sattanathanphd@gmail.com
*Corresponding Author: sattanathanphd@gmail.com (S.G.).

ABSTRACT

This study investigated the green synthesis of copper oxide nanoparticles (CuO NPs) using *Sargassum wightii* extract and their incorporation into starch/polyvinyl alcohol (PVA) electrospun nanoscaffolds for antimicrobial applications. The algal extract served as a reducing and stabilizing agent, yielding spherical CuO NPs with high colloidal stability (zeta potential: -120 mV). Characterization via UV-Vis spectroscopy, Fourier-transform infrared spectroscopy (FTIR), X-ray diffraction (XRD), and Scanning electron microscopy (SEM) confirmed the monoclinic crystalline structure of CuO NPs and their uniform dispersion within nanofibrous scaffolds. Antimicrobial testing at 50 µg/mL demonstrated that the CuO NP-loaded scaffolds exhibited superior activity against bacterial (*Escherichia coli, Klebsiella pneumoniae, Staphylococcus aureus, Citrobacter koseri*) and fungal (*Aspergillus niger, Penicillium* species) pathogens, with inhibition zones ranging from 19–23 mm, outperforming standalone CuO NPs (14–18 mm) and algal extract (10–15 mm). While less potent than ciprofloxacin (28–33 mm) and voriconazole (26–28 mm), the scaffolds showed enhanced efficacy due to synergistic effects. These findings highlight the potential of eco-friendly CuO NP-based nanoscaffolds as sustainable antimicrobial materials for biomedical applications.

KEYWORDS: *Sargassum wightii*, Green synthesis, CuO NPs, Starch/PVA-nanoscaffolds, Antimicrobial activity.

1. INTRODUCTION

The escalating need for antimicrobial solutions in biomedical applications has propelled investigations into innovative materials capable of countering pathogenic microbes [1]. Metal oxide nanoparticles (NPs) have emerged as prominent candidates due to their robust antimicrobial efficacy, compatibility with biological systems, and adaptability for integration into various substrates to facilitate controlled release [2]. Among these, copper oxide (CuO) NPs are particularly noteworthy, attributed to their distinctive physicochemical attributes such as elevated surface area, stability, and pronounced bactericidal and fungicidal activities [3]. Extensive studies have demonstrated the broad-spectrum antimicrobial prowess of CuO NPs against diverse bacterial and fungal pathogens, positioning them as promising agents in wound care, infection prevention, and drug delivery frameworks [4]. Nonetheless, conventional synthesis techniques for metal oxide NPs often entail the use of hazardous chemicals, substantial energy inputs, and stringent conditions, thereby raising concerns regarding their sustainability and environmental impact [5].

To mitigate these challenges, eco-friendly synthesis approaches leveraging natural resources have gained traction as viable alternatives for NP production [6]. These green synthesis methods employ plant extracts, microorganisms, or algae as reducing and stabilizing agents, offering an environmentally benign pathway for NP fabrication [7]. Marine algae, abundant and renewable, are rich in bioactive constituents, making them particularly suitable for such applications [8]. Specifically, marine macroalgae like *Sargassum wightii* are replete with bioactive compounds including polyphenols, flavonoids, and carotenoids, which can effectively function as natural reducing agents in the biosynthesis of metal oxide NPs [9].

S. wightii, a brown seaweed prevalent along the Indian coastline, has recently garnered attention for its potential in green synthesis methodologies [10]. The bioactive constituents inherent in this alga exhibit a spectrum of beneficial properties, encompassing antioxidant, antimicrobial, and anti-inflammatory effects, rendering it an ideal candidate for NP synthesis [11]. In the present study, extracts from *S. wightii* are utilized as green reducing agents to synthesize CuO NPs, which are subsequently incorporated into electrospun nanoscaffolds composed of

starch and polyvinyl alcohol (PVA) [12]. These CuO NP-infused nanoscaffolds are subjected to antimicrobial evaluations, aiming to develop sustainable antimicrobial materials suitable for biomedical applications [13].

Nanofibrous scaffolds have attracted considerable interest in tissue engineering and wound healing domains, owing to their high surface area, porosity, and structural resemblance to the extracellular matrix (ECM) [14]. Electrospinning stands out as a prevalent technique for fabricating such nanofibrous scaffolds, enabling the production of fibers with nanometer-scale diameters conducive to cellular interactions and tissue regeneration [15]. The amalgamation of starch, a biodegradable and biocompatible polysaccharide, with PVA, a synthetic polymer recognized for its water solubility and mechanical robustness, offers a promising platform for scaffold fabrication [16]. The integration of CuO NPs into these scaffolds augments their antimicrobial capabilities, culminating in a dual-functional system that not only fosters tissue regeneration but also impedes bacterial and fungal infections at the application site [17].

Embedding CuO NPs into nanofibrous scaffolds confers multiple advantages [18]. These NPs can effectively compromise bacterial cell membranes and suppress the proliferation of pathogenic microorganisms through the generation of reactive oxygen species (ROS), leading to oxidative damage in microbial cells [19]. Moreover, when incorporated into a scaffold matrix, the antimicrobial efficacy of CuO NPs is enhanced via sustained release at the infection locus [17]. This controlled release mechanism is particularly advantageous in wound healing contexts, where prolonged antimicrobial activity is imperative to avert secondary infections and facilitate tissue repair [20].

This investigation focuses on the green synthesis of CuO NPs employing *S. wightii* extracts and their subsequent integration into starch/PVA electrospun nanoscaffolds for antimicrobial applications. The green synthesis approach is adopted to circumvent the use of toxic chemicals and to promote a sustainable NP production methodology [5]. The synthesized CuO NPs undergo characterization through various techniques, including UV-Visible spectroscopy, Fourier-transform infrared (FTIR) spectroscopy, X-ray diffraction (XRD), and scanning electron microscopy (SEM), to ascertain their size, morphology, crystallinity, and dispersion within the nanofibrous scaffold matrix [21]. The antimicrobial efficacy of the CuO NP-loaded scaffolds is assessed against a spectrum of bacterial (*Escherichia coli*, *Klebsiella pneumoniae*, *Staphylococcus aureus*, *Citrobacter koseri*) and fungal (*Aspergillus niger*, *Penicillium* species) pathogens utilizing the agar well diffusion method [22]. Comparative analyses are conducted against the algae extract and standard antimicrobial agents, ciprofloxacin (for bacterial strains) and voriconazole (for fungal strains), serving as positive controls [23].

The principal aim of this study is to elucidate the potential of *S. wightii* extract-mediated green synthesized CuO NPs, incorporated into starch/PVA nanofibrous scaffolds, as eco-friendly and efficacious antimicrobial materials for biomedical applications [24]. By harnessing a natural and sustainable resource for NP synthesis and integrating it with electrospun nanofibers, the study endeavors to develop a material that addresses the escalating concerns of antimicrobial resistance while offering a safe, cost-effective, and environmentally sustainable alternative to conventional antimicrobial agents [25]. The successful fabrication of CuO NP-infused nanoscaffolds with enhanced antimicrobial properties could significantly impact the advancement of wound dressings, medical devices, and other biomaterials designed for infection control and tissue regeneration [26]. Furthermore, this research underscores the potential of marine macroalgae as renewable resources for the synthesis of functional nanomaterials, contributing to the progression of green nanotechnology and sustainable biomedical innovations.

2. MATERIALS AND METHODS

2.1. Materials

For this study, the macroalga *S. wightii* was collected from the coastal region of Rameswaram, Tamil Nadu, India, for the eco-friendly synthesis of CuO NPs. Copper (II) sulfate pentahydrate ($CuSO_4 \cdot 5H_2O$), used as the precursor, was procured from Sigma-Aldrich. PVA (molecular weight approximately 115,000) served as the primary polymer for electrospinning, while starch from a local supplier was used to enhance scaffold features. All other solvents and reagents, such as ethanol and Milli-Q water, were of analytical grade and obtained from Merck and Sigma-Aldrich. The electrospinning process utilized a HOLMARC HO-NFES-040 unit equipped with a syringe pump. Characterization instruments included a UV-Vis spectrophotometer (VIS SPEC V-730), FT-IR spectrometer (Spectrum Two, PerkinElmer), XRD (Bruker D8 Advance), SEM (JSM-IT800 NANO), and zeta potential and Dynamic light scattering (DLS) analyzer (Malvern Zetasizer Ultra). Thermal analyses were carried out using a Thermogravimetric analysis (TGA) 8000 (PerkinElmer).

2.2. Marine macroalgae collection

Fresh *S. wightii* samples were gathered from coastal waters near Rameswaram. The collected *S. wightii* was taxonomically identified and authenticated by Dr V. Veeragurunathan, CSIR-CSMCRI-Marine Algal Research Station, Mandapam Camp 623519, Tamil Nadu, India. A voucher specimen was prepared and deposited at the Herbarium of the CSIR-CSMCRI-Marine Algal Research Station, under the accession number: SI–2025–RMM–017. This authentication ensures botanical accuracy and standardization of the study material. The algae were initially washed with running tap water to eliminate debris and surface organisms, followed by a rinse with distilled water for final cleaning. About 100 grams of the cleaned algae were chopped into small pieces and dried under ambient conditions for around 14 days. The dried material was then pulverized using a mechanical grinder and preserved in airtight containers for later use.

2.3. Ultrasonic extraction

To isolate bioactive components, 2 g of powdered *S. wightii* was mixed with 50 mL of Milli-Q water in a 100 mL beaker. The extraction was performed via ultrasonic-assisted technique using a LABQUEST ultrasonic cleaner (Borosil; Serial No. 941032329018) at 60°C for 45 minutes. The extract was filtered using sterile Whatman No. 1 filter paper. The clear filtrate was collected and stored at 10°C for immediate use, while for extended storage, the extract was lyophilized into a dry powder using a laboratory freeze-dryer [27].

2.4. Green synthesis of CuO NPs

Biosynthesis of CuO NPs was performed using the *S. wightii* extract. Specifically, 50 mL of 0.1 M $CuSO_4 \cdot 5H_2O$ was combined with 10 mL of algal extract (prepared by dissolving 10 mg in 10 mL Milli-Q water) in a 5:1 ratio. This solution was stirred at 650 rpm and maintained at 60°C for 2 hours. A visible change in color from blue to bluish-green confirmed NP formation. The synthesized NPs were rinsed three times with double-distilled water at the same temperature and agitation conditions to remove residual reactants. Final products were freeze-dried for 48 hours and stored as dry powders for characterization and fabrication [28].

2.5. Preparation of CuO-embedded electrospun PVA/starch scaffolds

A 15% (w/w) aqueous PVA solution was prepared under constant stirring until fully dissolved. To this, 100 mg of starch and 100 mg of synthesized CuO NPs were added, followed by stirring at 50°C for 2.5 hours for thorough dispersion. The homogeneous solution was transferred to a syringe equipped with a 0.84 mm internal diameter needle and electrospun using a HOLMARC HO-NFES-040 system, supported by a HMPSKV30 high-voltage power supply (0–30 kV, 0.5 mA). Electrospinning was carried out at 11.5 kV, with a needle-to-collector gap of 12.3 cm and flow rate of 0.4 mL/h for 6–8 hours at ambient temperature to produce nanofibrous mats [29, 30].

2.6. Physicochemical evaluation

2.6.1. UV-visible spectroscopy

UV-Vis spectroscopy was applied to verify NP formation and analyze optical characteristics of both *S. wightii* extract and the CuO NPs. Spectra were recorded using VIS SPEC V-730 over 200–800 nm, with deionized water as the reference. Presence of surface plasmon resonance (SPR) peaks indicated successful NP synthesis and interactions within the scaffold matrix [31].

2.6.2. FTIR spectral analysis

FTIR spectra were acquired using the ATR mode of PerkinElmer Spectrum Two to identify functional groups and molecular interactions. Spectra were recorded from 4000 to 400 cm^{-1} using 64 scans per sample at a resolution of 4 cm^{-1}. Peaks corresponding to hydroxyl, carbonyl, amide, and metal-oxygen bonds were analyzed in both the NPs and composite scaffolds [32].

2.6.3. XRD analysis

Crystallographic studies of CuO NPs and scaffolds were conducted using Bruker D8 Advance with CuKα radiation (wavelength $\lambda = 1.5406$ Å), operated at 40 kV and 40 mA. Diffraction patterns were recorded over $2\theta = 5°$ to 90° at 0.029649° increments. Characteristic peaks were matched to monoclinic CuO, and peak shifts were used to infer NP-polymer interactions [33].

2.6.4. SEM analysis

SEM was utilized for surface morphology, fiber distribution, and NP dispersion assessment using a JEOL JSM-IT800 NANO. Samples were sputter-coated with gold to prevent charging. High-resolution images provided insights into NP embedding and nanofiber alignment [27].

2.6.5. TGA

Thermal properties of CuO-incorporated scaffolds were analyzed with PerkinElmer TGA 8000. Around 5 mg of sample was heated from room temperature to 550°C at 15°C/min under nitrogen. Weight loss data were used to evaluate moisture content, decomposition, and thermal resistance of the materials [34].

2.6.6. DLS and zeta potential measurements

NP size and zeta potential were measured with Malvern Zetasizer Ultra using DLS. These parameters reflected particle stability and surface charge. Higher absolute zeta potential values signified better colloidal stability, important for biomedical applicability [35].

All experimental and processed characterization data are publicly accessible via the Mendeley Data repository (DOI: 10.17632/vf8822rd8j.1), supporting transparency and reproducibility.

2.7. Antimicrobial testing

Antibacterial and antifungal activities of *S. wightii* extract, CuO NPs, and PVA/starch electrospun scaffolds (50 µg/mL each) were evaluated using agar well diffusion. The test organisms included *Escherichia coli*, *Klebsiella pneumoniae*, *Staphylococcus aureus*, *Citrobacter koseri*, *Aspergillus niger*, and *Penicillium* sp. Bacterial cultures were standardized to 0.5 McFarland (approx. 1.5×10^8 CFU/mL) and seeded on Mueller-Hinton agar, while fungi were cultured on Sabouraud dextrose agar. Wells (6 mm diameter) were filled with 50 µL of each sample. Ciprofloxacin and voriconazole were used as bacterial and fungal controls, respectively. After 30 minutes of pre-diffusion, plates were incubated at 37°C for 24 h (bacteria) and 28°C for 48 h (fungi). Inhibition zones (mm) were recorded. All tests were conducted in triplicate for accuracy [36, 37].

2.8. Data analysis

Statistical analysis was carried out using SPSS (Version 25.0) and GraphPad Prism (Version 9.0). Results are presented as mean ± standard deviation (SD) from three independent experiments. One-way ANOVA followed by Tukey's and Dunnett's post hoc tests were used for comparison. Significance was set at $p < 0.05$. Normality was verified using the Shapiro-Wilk test, and data were log-transformed if non-normal. Correlations between variables were evaluated using Pearson's correlation coefficient. A 95% confidence level was maintained throughout the analysis [38].

3. RESULTS AND DISCUSSION

3.1. UV–visible spectroscopy

The UV-Visible spectroscopy analysis (Fig. 1) of the aqueous *S. wightii* extract and the green-synthesized CuO NPs revealed distinct absorption peaks that confirm NP formation and their optical properties. The extract exhibited a significant absorption peak at 346 nm, indicative of bioactive compounds such as polyphenols or flavonoids, which may serve as reducing and stabilizing agents during synthesis. The CuO NPs exhibited a pronounced absorption peak at 292 nm, corresponding to the surface plasmon resonance (SPR) phenomenon, confirming the successful formation of CuO NPs. Additionally, a broader absorption band in the visible region (400–800 nm) was observed, suggesting NP aggregation or interactions within the composite matrix. Measurements, taken with a VIS SPEC V-730 spectrophotometer (200–800 nm range), using deionized water as a blank, demonstrated the effective synthesis of CuO NPs through green methods and their stable optical properties. The absence of impurities or secondary peaks further supports the purity of the synthesized NPs. These results are consistent with the typical SPR behavior seen in metal oxide NPs, highlighting the potential of *S. wightii* extract as a sustainable reducing agent for CuO NP synthesis [39-45].

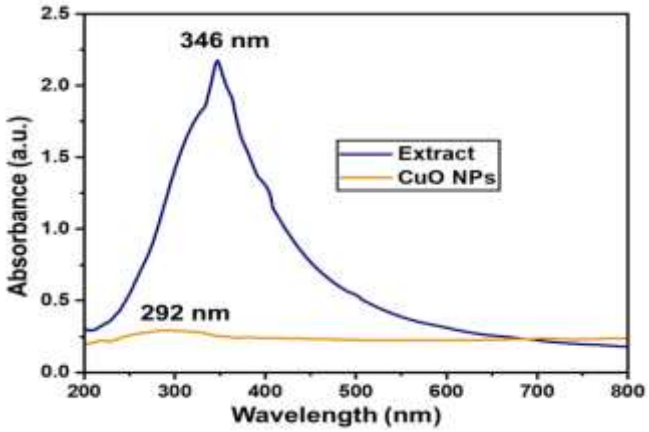

Fig. 1. UV–Visible spectral profiles of algal extract and CuO NPs.

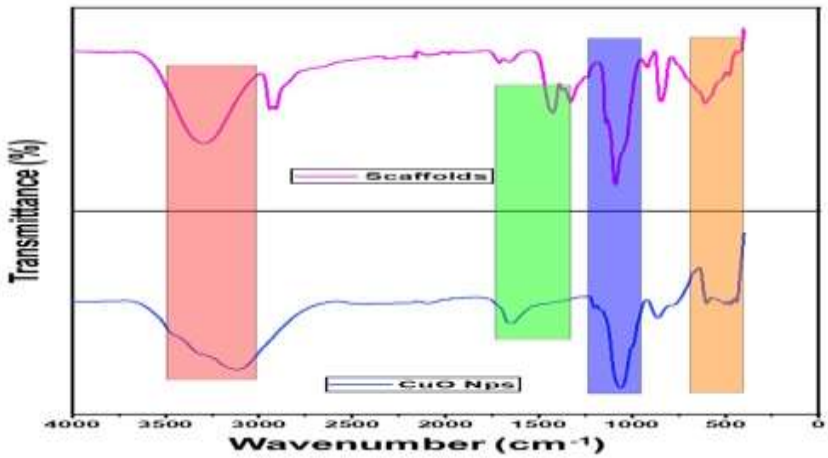

Fig. 2. FTIR spectra of CuO NPs and their incorporation into nanoscaffolds.

3.2. FTIR spectroscopy analysis

FTIR analysis (Fig. 2) of the CuO NPs and starch/PVA electrospun nanoscaffolds was performed using ATR mode on a PerkinElmer Spectrum Two instrument (range 4000–400 cm^{-1}, resolution 4 cm^{-1}, and 64 scans). The CuO NPs spectrum displayed 11 distinct peaks, suggesting the presence of functional groups involved in stabilization and metal-oxygen bonding. The nanoscaffold spectrum showed notable absorption bands at 3298.42 cm^{-1} (O–H/N–H stretching, indicating hydroxyl or amine groups), 2924.17 cm^{-1} (C–H stretching of aliphatic chains), 1710.48 cm^{-1} (C=O stretching of carbonyl groups), 1426.82 cm^{-1} (C–H bending or COO^- symmetric

stretching), and 1097.57 cm^{-1} (C–O–C or Si–O–Si vibrations). Additional peaks at 1329.64 cm^{-1}, 919.55 cm^{-1}, and 843.63 cm^{-1} may be associated with C–N stretching, P–O–C bonds, or metal-oxygen (Cu–O) vibrations, confirming the incorporation of CuO NPs into the scaffold. The absence of impurities and shifts or broadening of certain peaks suggest successful interactions between the NPs and scaffold components, likely via hydrogen bonding or electrostatic forces. These findings underline the scaffold's functional group diversity and the successful itegration of CuO NPs, which may affect the material's mechanical, biological, and catalytic properties [46-51].

3.3. XRD analysis

XRD analysis (Fig. 3) of the synthesized CuO NPs and starch/PVA electrospun nanoscaffolds was performed with a Bruker D8 Advance diffractometer using CuKα radiation (λ = 1.5406 Å, 40 kV, 40 mA) over a 2θ range of 5°–90° (step size: 0.029649°). The CuO NPs exhibited 32 distinct diffraction peaks, with prominent reflections at 16.386° (5.405 Å), 22.406° (3.965 Å), 24.107° (3.689 Å), 31.894° (2.804 Å), 32.745° (2.733 Å), 38.307° (2.348 Å), and 48.057° (1.892 Å), corresponding to the monoclinic tenorite phase of CuO (JCPDS 05-0661). The high-intensity peaks at 22.406° and 24.107° (relative intensities: 80.2% and 100%, respectively) confirmed the high crystallinity, while peak broadening indicated nanoscale crystallite dimensions. The nanoscaffolds showed a semi-crystalline structure with 45.3% crystallinity and 54.7% amorphous content. Key peaks at 29.372° (3.038 Å), 38.502° (2.336 Å), and 44.687° (2.026 Å) suggested CuO NP presence in the scaffold matrix, as evidenced by peak shifts (e.g., 38.502° vs. 38.307° in pure CuO NPs) and reduced intensities, signifying NP-polymer interactions. The FWHM values (e.g., 0.130°–0.341° for scaffolds vs. 0.115°–0.580° for CuO NPs) reflected differences in crystallite size and strain. The absence of impurity peaks confirmed phase purity in both systems, while the broader peaks in the scaffold suggested reduced crystallinity due to polymer incorporation. These results indicate successful CuO NP synthesis and incorporation into the scaffold, maintaining structural integrity and tailored crystallinity for biomedical or catalytic applications [52-58].

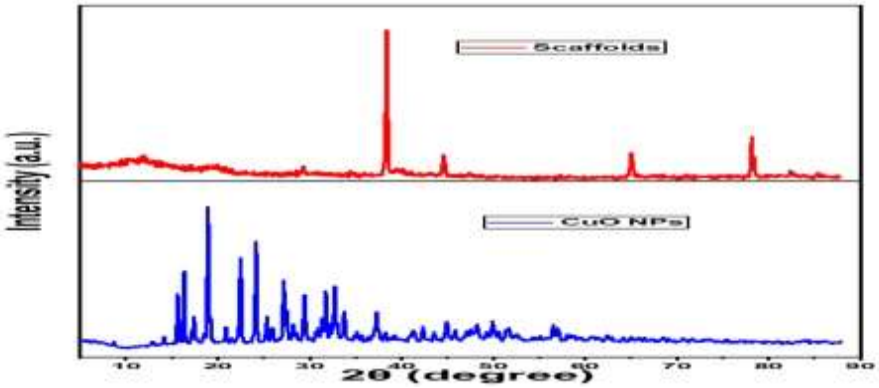

Fig. 3. XRD patterns of synthesized CuO NPs and CuO-loaded scaffolds.

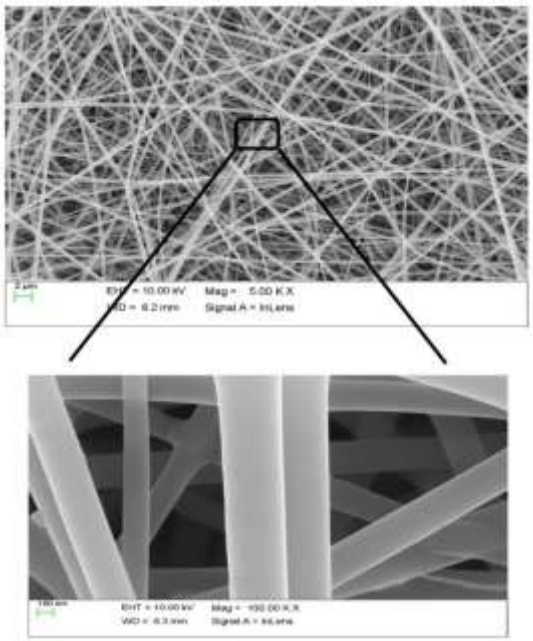

Fig. 4. SEM analysis of synthesized CuO NPs and CuO-loaded scaffolds.

3.4. SEM analysis

SEM analysis (Fig. 4) of the CuO NPs and starch/PVA electrospun nanoscaffolds was carried out using a JEOL JSM-IT800 NANO system, with samples sputter-coated with gold to minimize charging effects. High-resolution micrographs revealed that the CuO NPs exhibited a uniform spherical morphology with an average size of 130–160 nm, indicating successful synthesis with minimal aggregation. The starch/PVA electrospun scaffolds presented a highly porous, interconnected fibrous network, with fiber diameters ranging from 150–200 nm, indicating optimal electrospinning conditions. The CuO NPs were evenly distributed across the scaffold fibers, confirming effective integration without clumping, which is essential for maintaining structural integrity and functionality. The nanofibers exhibited smooth surfaces with occasional bead-free alignment, suggesting consistent polymer jet stability during electrospinning. The SEM results highlight the scaffold's nanofibrous structure, which facilitates cell adhesion and nutrient diffusion, while the homogeneous distribution of CuO NPs within the matrix enhances potential antimicrobial or catalytic properties. These findings underscore the suitability of the composite scaffold for applications in tissue engineering or drug delivery, where controlled morphology and NP distribution are crucial [59-64].

3.5. TGA

TGA (Fig. 5) of the starch/PVA electrospun nanoscaffolds was conducted using a PerkinElmer TGA 8000 system under nitrogen flow, with a 5.518 mg sample heated from room temperature to 550°C at a rate of 15°C/min. The thermogram exhibited a multi-stage degradation profile, beginning with an initial weight loss below 150°C, attributed to moisture evaporation. The primary degradation occurred between 220.95°C (onset) and 382.16°C (end), with a peak at 322.94°C, corresponding to the thermal decomposition of starch and PVA polymer chains, including breakdown of hydroxyl groups and glycosidic linkages. A total mass loss of 37.126% in this region indicated significant polymer degradation, while the sharp peak suggested rapid decomposition. No residual mass data was noted beyond 382.16°C, but the absence of additional peaks implied that the remaining scaffold components or CuO NPs remained stable at higher temperatures. The results indicate moderate thermal stability for the scaffold up to ~220°C, making it suitable for applications requiring processing or sterilization below this threshold. The degradation profile aligns with typical starch/PVA-based materials, and CuO integration likely enhances thermal resistance, although further analysis is necessary to quantify residual ash or NP effects [65-71].

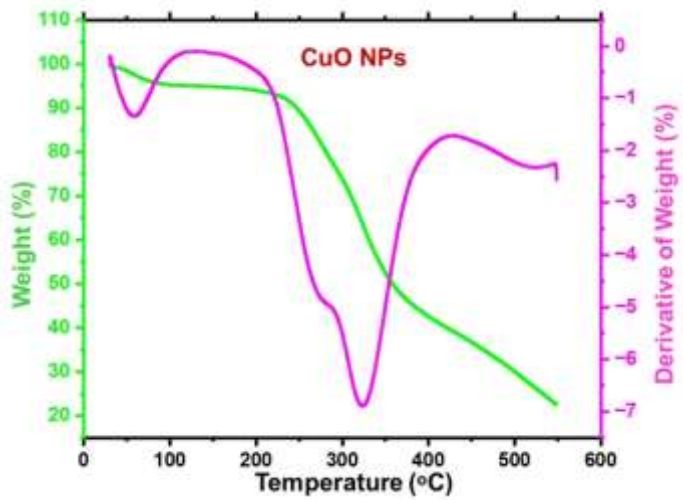

Fig. 5. Thermal degradation behavior of CuO-incorporated nanoscaffolds.

3.6. Zeta potential and particle size analysis

DLS and zeta potential analysis of the CuO NPs were conducted using a Malvern Zetasizer Ultra to assess their colloidal stability and size distribution in aqueous suspension. The DLS results revealed a monodisperse distribution with an average hydrodynamic diameter of 146.1 nm (Fig. 6), indicating the formation of well-dispersed NPs. Zeta potential measurements revealed a highly negative surface charge of -120 mV (Fig. 7), suggesting strong electrostatic repulsion between particles, preventing aggregation and ensuring excellent colloidal stability. The high absolute zeta potential value (> ±30 mV) confirms that the CuO NPs possess long-term stability in suspension, which is essential for biomedical and catalytic applications requiring uniform dispersion. The narrow size distribution and strong negative charge further indicate successful synthesis and surface modification, likely due to capping agents or functional groups introduced during the green synthesis process. These results demonstrate that the CuO NPs possess optimal physicochemical properties for stable dispersion in aqueous environments [72-76].

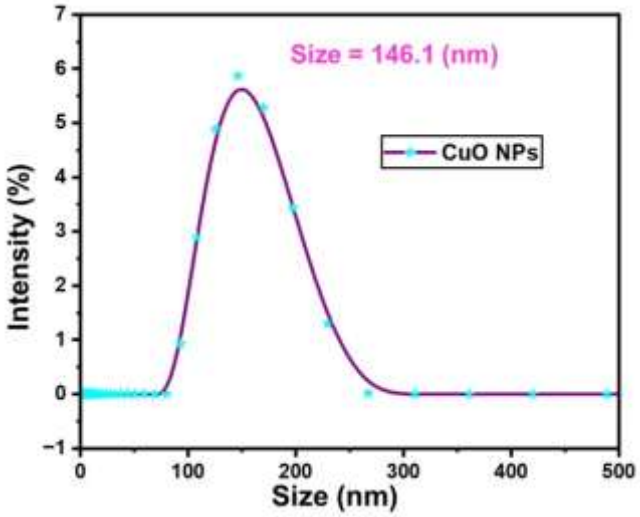

Fig.6. DLS particles size analysis of CuO NPs

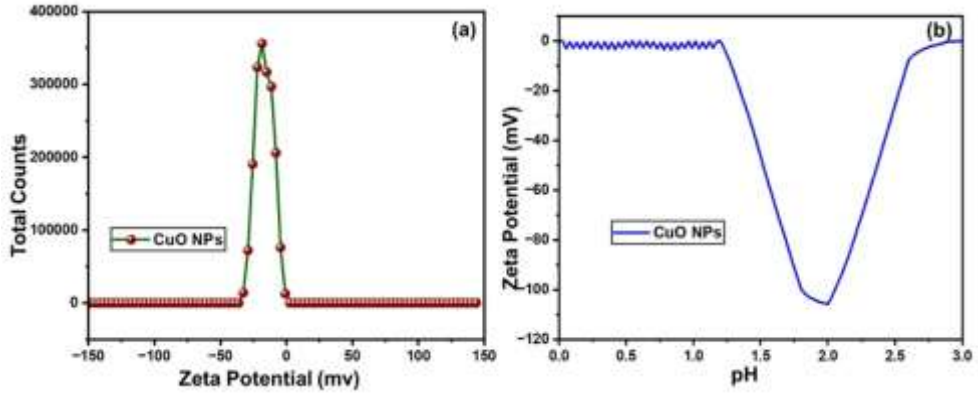

Fig.7. Zeta-potential analysis of CuO NPs

3.7. Antimicrobial activity

The antimicrobial activity of *S. wightii* extract, CuO NPs, and starch/PVA electrospun nanoscaffolds was evaluated at 50 µg/mL against pathogenic bacteria (*Escherichia coli*, *Klebsiella pneumoniae*, *Staphylococcus aureus*, *Citrobacter koseri*) and fungi (*Aspergillus niger*, *Penicillium* species) (Table 1). The algal extract demonstrated moderate inhibition, with zones ranging from 10±0.14 mm (*S. aureus*) to 15±0.26 mm (*Penicillium* species). CuO NPs exhibited slightly enhanced antibacterial activity (14±0.31 mm to 17±0.18 mm) and antifungal effects (17±0.11 mm to 18±0.16 mm). Notably, the starch/PVA nanoscaffolds embedded with CuO NPs showed superior antimicrobial performance, with inhibition zones of 22±0.16 mm (*E. coli*), 21±0.36 mm (*K. pneumoniae*), 19±0.13 mm (*S. aureus*), 21±0.24 mm (*C. koseri*), 23±0.14 mm (*A. niger*), and 23±0.16 mm (*Penicillium* species). While the nanoscaffolds outperformed both the extract and standalone CuO NPs, their efficacy remained below the positive controls ciprofloxacin (28–33 mm) and voriconazole (26–28 mm). These results highlight the synergistic antimicrobial potential of CuO NP-loaded nanoscaffolds, suggesting their promise as biocompatible alternatives for combating microbial pathogens [77, 78].

Table 1: Antimicrobial activity of *S. wightii* extract, CuO NPs, and starch/PVA electrospun nanoscaffolds at concentration of 50 µg/mL against various pathogenic organisms.

S. No	Organisms	Zone of inhibition (mm)				
		Ciprofloxacin (Antibiotic)	Voriconazole (Antifungal)	Algal Extract	CuO NPs	Nano-scaffolds
1.	*Escherichia coli*	33±0.58	-	13±0.15	17±0.18	22±0.16
2.	*Klebsiella pneumoniae*	30±0.14	-	11±0.27	15±0.15	21±0.36
3.	*Staphylococcus aureus*	28±0.32	-	10±0.14	14±0.31	19±0.13
4.	*Citrobacter koseri*	29±0.47	-	11±0.42	15±0.12	21±0.24
5.	*Aspergillus niger*	-	26±0.65	13±0.11	17±0.11	23±0.14
6.	*Penicillium* species	-	28±0.39	15±0.26	18±0.16	23±0.16

5. CONCLUSION

This study successfully demonstrated the green synthesis of CuO NPs using *S. wightii* extract and their incorporation into starch/PVA electrospun nanoscaffolds for antimicrobial applications. The phytochemical-rich algal extract served as an effective reducing and capping agent, producing spherical CuO NPs (130–160 nm) with high colloidal stability (zeta potential: -120 mV). Comprehensive characterization confirmed the monoclinic crystalline structure of CuO NPs and their uniform dispersion within nanofibrous scaffolds (150–200 nm diameter). Antimicrobial evaluation revealed that the CuO NP-loaded scaffolds exhibited superior activity against bacterial (*Escherichia coli*, *Klebsiella pneumoniae*, *Staphylococcus aureus*, *Citrobacter koseri*) and fungal (*Aspergillus niger*, *Penicillium* species) pathogens, with inhibition zones of 19–23 mm, outperforming standalone CuO NPs (14–18 mm) and algal extract (10–15 mm). While less potent than conventional antibiotics, the scaffolds demonstrated enhanced efficacy due to synergistic effects between CuO NPs and the polymer matrix. These findings highlight the potential of eco-friendly CuO NP-based nanoscaffolds as sustainable antimicrobial materials for biomedical applications, offering a promising alternative to combat microbial resistance. Future research could explore their use in wound dressings or tissue engineering scaffolds.

Funding: Not available for this study

Ethical Declaration: Not Applicable

Data Availability Statement: The full dataset of physiochemical characterization associated with this work is published in Mendeley Data [Dataset] Eco-conscious biomaterial design: Analytical insights into starch nanoscaffolds with green-engineered copper oxide nanoparticles using marine Sargassum wightii extract (DOI: 10.17632/vf8822rd8j.1). Disclosure: The material characterization data and figures (e.g., UV, SEM, FTIR, XRD, TGA, Zeta Potential and particle sizer) presented here were generated from a common dataset and are being reused across multiple related studies on nanomaterials. All biological analyses and conclusions are original to each manuscript.

Conflicts of Interest: The authors declare no conflicts of interest.

REFERENCES

[1] Natarajan PM. Computational Studies on Recent Congeners of Fluoroquinolones and Nitroimidazoles for Their Use in Periodontal Therapy. Journal of Pharmacy and Bioallied Sciences. 2024; 16(5): S4731-S4740.
[2] Yadalam PK, Arumuganainar D, Natarajan PM, Ardila CM. Artificial intelligence-powered prediction of AIM-2 inflammasome sequences using transformers and graph attention networks in periodontal inflammation. Scientific Reports. 2025; 15: 8733.
[3] Yadalam PK, Chatterjee S, Natarajan PM, Ardila CM. Comparison of light gradient boosting and logistic reg ression for interactomic hub genes in Porphyromonas gingivalis and Fusobacterium nucleatum-induced periodo ntitis with Alzheimer's disease. Frontiers in Oral Health. 2025; 6:1463458.
[4] Natarajan PM, Bhuminathan S, Leela B, Bindu K, Loganathan K, Ramachandran V. Smoking and its Role in Oral Cancer. Journal of Pharmacy and Bioallied Sciences 16(5): S4242-S4244.
[5] Yadalam PK, Natarajan PM, Ardila CM. Variational graph autoencoder for reconstructed transcriptomic data associated with NLRP3 mediated pyroptosis in periodontitis. Scientific Reports. 2025; 15: 1962.
[6] Guan T, Gong J, Lin J, Palanisamy CP, Jinjin Pei J, El-Aty AMA. Machine learning-driven multimodal optimization of selenium biotransformation and flavor profiling in fermented apple–Yacon functional beverages. Innovative Food Science & Emerging Technologies. 2025; 105: 104198.
[7] Natarajan SR, Krishnamoorthy R, Alshuniaber MA, Alsulami TS, Gatasheh MK, Rajagopal P, Palanisamy CP, Govindan R, Veeraraghavan VP, Jayaraman S. ABCE1 facilitates tumour progression via aerobic glycolysis and inhibits cell death in human colorectal cancer cells through the p53 signalling pathway. Scientific Reports. 2025; 15: 24674.
[8] Huang Y, Guo H, Liu Y, Jin W, Palanisamy CP, Pei J, Oz F, El-Aty AMA. Effects of Natural Polysaccharides on the Gut Microbiota Related to Human Metabolic Health. Molecular Nutrition & Food Research. 2025; 69:e202400792.
[9] Poornima K, Meenakshi K.C, Manikandan V.R, Shankari G, Prabhu D, Rathi M.A, Palanisamy CP, Balaji R, Gopalakrishnan V.K. Exploring the anticancer potential of Jerantinine A from *Tabernaemontana coronaria* against prostate, breast, and ovarian cancers: A computational approach. *Journal of Complementary and Integrative Medicine*, 2025 22(2): 363–372.
[10] Palanisamy CP, Poompradub S, Sansanaphongpricha K, Jayaraman S, Subramani K. Faridah Sonsudin gGreen synthesis of Nigella sativa-mediated silver nanoparticles for enhanced antibacterial activity and wound healing: Mechanistic insights and biomedical applications. Environmental Nanotechnology, Monitoring & Management. 2025; 24: 101085.

[11] Surendran N, Raju MV, Chandrasekaran MK, Ahalliya RM, Palanisamy CP, Chandrasekaran G, Kanniappan GV. Physicochemical characterization of starch from Maranta arundinacea L.(arrowroot) rhizomes and its inhibition of COX-2: In vivo validation. Bioactive Carbohydrates and Dietary Fibre. 2025; 33: 100465.
[12] Kannappan P, Chandrasekaran MK, Raju MV, Gopalakrishnan S, Dhamodharan P, Ahalliya RM, Palanisamy CP, Raju B, Kanniappan GV. Exploring the anticancer potential of Jerantinine A from Tabernaemontana coronaria against prostate, breast, and ovarian cancers: a computational approach. Journal of Complementary and Integrative Medicine. 2025; 22(02): 363-372.
[13] Pei J, Kumarasamy RV, Jayaraman S, Kanniappan GV, Long Q, Palanisamy CP. Quercetin-functionalized nanomaterials: Innovative therapeutic avenues for Alzheimer's disease management. Ageing Research Reviews. 2025; 104: 102665.
[14] Jayaraman S, Prasad M, Natarajan SR, Krishnamoorthy R, Alshuniaber MA, Gatasheh MK, Veeraraghavan VP, Rajagopal P, Palanisamy CP. Molecular mechanisms underlying the effects of beta-sitosterol on TGF-β1/Nrf2/SIRT1/p53-mediated signaling in the kidney of a high-fat diet and sucrose-induced type-2 diabetic rat. Chemico-Biological Interactions. 2025; 411: 111443.
[15] Huang Y, Guo H, Liu Y, Jin W, Palanisamy CP, Pei J, Oz F, El-Aty AMA. Effects of Natural Polysaccharides on the Gut Microbiota Related to Human Metabolic Health. Molecular Nutrition & Food Research. 2025; e202400792.
[16] Prabhakaran P, Palanisamy CP, Shanmugam A, Damodharan P, Swaminathan H, Devaraj D, Ahalliya RM, Kanniappan GV. Isolation, structural characterization, and molecular docking studies on the bioactive compound from n-Hexane extract of Emilia sonchifolia (L.) DC against the pancreatic cancer target Aurora 2 Kinase. Journal of Complementary and Integrative Medicine. 2024; 22(1): 0290.
[17] Jiang H, Kumarasamy RV, Pei J, Raju K, Kanniappan GV, Palanisamy CP. Integrating engineered nanomaterials with extracellular vesicles: Advancing targeted drug delivery and biomedical applications. Frontiers in Nanotechnology. 2024; 6: 1513683.
[18] Guo H, Liu Y, Wan T, Song D, Palanisamy CP, Geng J, Pei J, Özmen S, El-Aty AMA. Toward personalized cancer management: Role of precision nutrition–diet interventions. Journal of Functional Foods. 2024; 123: 106584.
[19] Natarajan SR, Krishnamoorthy R, Alshuniaber MA, Al-Anazi KM, Farah MA, Rajagopal P, Palanisamy CP, Veeraraghavan VP, Jayaraman S. Identification of FOXM1 as a novel protein biomarker and therapeutic target for colorectal cancer progression: Evidence from immune infiltration and bioinformatic analyses. International Journal of Biological Macromolecules. 282 (Part 4): 137201.
[20] Rajendran MS, Jayaraman S, Khan JM, Jasmine S, Prabhakaran RK, Raju MV, Chandrasekaran MK, Ahalliya RM, Kannappan P, Palanisamy CP, Kanniappan GV. Investigating the colon toxicity and carcinogenic role of monosodium glutamate compared with Dimethylhydrazine in male Wistar rats: Exploring the link to childhood colon cancer risk. Journal of King Saud University - Science. 2024; 36(11): 103507.
[21] Kumarasamy RV, Natarajan P, Umapathy VR, Roy JR, Rab SO, Saeed M, Panagal M, Mironescu M, Srinivasan GP, Palanisamy CP. Clinical Applications and Therapeutic Potentials of Advanced Nanoparticles: A Comprehensive Review on Completed Human Clinical Trials. Frontiers in Nanotechnology. 2024; 6:1479993.
[22] Jin W, Pei JJ, Roy JR, Jayaraman S, Ahalliya RM, Kanniappan GV, Mironescu M, Palanisamy CP. Comprehensive review on single-cell RNA sequencing: A new frontier in Alzheimer's disease research. Ageing Research Reviews. 2024; 274: 102454.
[23] Pei J, Palanisamy CP, Jayaraman S, Natarajan PM, Umapathy VR, Roy JR, Panagal M, Jayaraman S. Curcumin-loaded polymeric nanomaterials as a novel therapeutic strategy for Alzheimer's disease: A comprehensive review. Ageing Research Reviews. 2024; 99: 102393.
[24] Pei J, Palanisamy CP, Jayaraman S, Natarajan PM, Umapathy VR, Roy JR, Thalamati D, Ahalliya RM, Kanniappan GV, Mironescu M. A comprehensive review on starch-based Sustainable Edible Films Loaded with Bioactive Components for Food Packaging. International Journal of Biological macromolecules. 2024; 274 (Part-1): 133332.
[25] Palanisamy CP, poompradub S, Sansanaphongpricha K, Subramani K, Sonsudin F. Increased expression levels of PDGF and VEGF magnify the wound healing potential facilitated by biogenic synthesis of silver nanoparticles. Nano-Structures & Nano-Objects. 2024; 39: 101236.
[26] Pei J, Palanisamy CP, Jayaraman S, Natarajan PM, Umapathy VR, Roy JR, Thalamati D, Ahalliya RM, Kanniappan GV, Mironescu M. Proteomics Profiling of Extracellular Vesicle for Identification of Potential Biomarkers in Alzheimer's Disease: A Comprehensive Review. Ageing Research Reviews. 2024; 99: 102359.
[27] Ganesan A, Kumar NG, Natarajan PM. Solanum trilobatum leaf extract-derived silver nanoparticles downregulate the PI3K/AKT/mTOR signaling pathway and attenuate oral squamous cell carcinoma cell proliferation. Journal of Herbmed Pharmacology. 2024; 13(2): 300-307.
[28] Perumal MKK, Renuka RR, Subbiah SK, Natarajan PM. Artificial intelligence-driven clinical decision support systems for early detection and precision therapy in oral cancer: a mini review. Frontiers in Oral Health. 2025; 6: 1592428.
[29] Ramesh E, Ganesan A, Lakshmi KC, Natarajan PM. Artificial intelligence-based diagnosis of oral leukoplakia using deep convolutional neural networks Xception and MobileNet-v2. Frontiers in Oral Health. 2025; 6: 1414524.

[30] Ganesan A, Kumar NG, Natarajan PM. Anticancer activity of silver nanoparticles synthesized from aqueous leaf extract of Solanum trilobatum (Purple fruit pea eggplant) on human oral cancer cells. Journal of Herbmed Pharmacololgy. 2024; 13(2): 260-268.
[31] Natarajan PM, Swamikannu B, Sivaraman NM, Stylin AGSQ. Prevention of Oral Cancer: A Comprehensive Guide. Journal of Pharmacy and Bioallied Sciences. 2024; 16(5): S4239-S4241.
[32] Umapathy V, Dhanavel A, Kesavan R, Natarajan PM, Bhuminathan S, Vijayalakshmi P. Anticancer Potential of the Principal Constituent of Piper nigrum, Piperine: A Comprehensive Review. Cureus. 2024; 16(2): e54425.
[33] Umapathy VR, Swamikannu B, Natarajan PM, Devi R, Nandini MS, Vimalarani, Vijayalakshmi P. In Silico Molecular Docking of Ocimum sanctum Phytochemicals: Targeting Key Biomarkers in Oral Cancer. Journal of Pharmacy and Bioallied Sciences. 2024; 16(5): S4792-S4799.
[34] Natarajan PM, Bhuminathan S, Rajan R, Bindu K, Loganathan K, Veerakumar R. The Crucial Role of Smoking Cessation in Preventing Oral Cancer. Journal of Pharmacy and Bioallied Sciences. 2024; 16(5): S4245-S4247.
[35] Swamikannu B, Umapathy VR, Natarajan PM, Nandini MS, Stylin AGSQ, Vimalarani V, Rajinikanth S. Unlocking the Therapeutic Benefits of Artemisia Annua: A Comprehensive Overview of its Medicinal Properties. Journal of Pharmacy and Bioallied Sciences. 2024; 16(5): S4248-S4253.
[36] Pei JJ, Perumal NC, Meng P, Long Q, Palanisamy CP. AI-assisted FTIR spectroscopic profiling of exosomes: Emerging frontiers in early detection of Alzheimer's disease. Ageing Research Reviews. 2026; 103311.
[37] Raja FSD, Abraham L, Rangasamy K, Saikia K, Rathankumar AK, Mironescu M, Mironescu I, Palanisamy CP, Kanniappan GV. Next-Generation Microbiome Therapeutics: Psychobiotics and Fecal Microbiota Transplants (FMT) for Mental Health Treatment. Frontiers in Cellular and Infection Microbiology. 2026; 16: 1719357.
[38] Subramani K, Srinivasan S, Shanmugam P, Palanisamy CP, Sonsudin F, Poompradub S. Sustainable phytochemical mediated-ZnO nanoparticles derived from Crescentia cujete for toxicological evaluation and multifunctional environmental applications. Environmental Nanotechnology, Monitoring & Management. 2026; 26: 101180.
[39] Kunamalla RP, Panagal M, Palanisamy CP. Green-engineered multiscale starch/PVA nanofibrous scaffolds embedded with CuO nanoparticles from Sargassum ilicifolium for potent antimicrobial performance. Genetics and Molecular Research. 2026; 25(13s): 1-9.
[40] Dharmaprakash S, Gunasekaran VP, Sivaramakrishnan R, Kanniappan GV, Jayaraman S, Mironescu M, Rajabathar JR, Mironescu ID, Palanisamy CP. Marine macroalgae-mediated ultrasonic-assisted green synthesis of CuO nanoparticles embedded in starch/PVA electrospun nanoscaffolds for in vitro α-amylase and α-glucosidase inhibitory activity. Scientific Reports. 2026; 16: 26243.
[41] Surendran N, Chandrasekaran G, Raju MV, Chandrasekaran MK, Ahalliya RM, Palanisamy CP, Kanniappan GV, Arcot R, Alharbi NS, Thiruvengadam M. Anti-inflammatory potential of ethanolic extract of Maranta arundinacea L.: Insights from COX-2 modulation and oxidative stress analysis. South African Journal of Botany. 2026; 195: 142-151.
[42] Pei J, Senthilkumar MV, Hessini K, Subramaniyam S, Sivaramakrishnan R, Kanniappan GV, Jayaraman S, Palanisamy CP. Green fabrication of starch/PVA/CuO nanoscaffolds using marine macroalgae extract for enhanced anti-inflammatory activity. Sustainable Chemistry and Pharmacy. 2026; 51: 102397.
[43] Balasubramanian V, Loganathan L, Muthuswamy K, Viswanathan TM, Raju MV, Chandrasekaran MK, Ahalliya RM, Poorasamy J, Palanisamy CP, Dominic S, Kanniappan GV. Anticancer therapeutic efficacy of PEGylated β-galactosidase from Aspergillus terreus in DMBA-induced breast cancer: Toxicological, molecular and histopathological evaluation in Wistar rats. International Journal of Biological Macromolecules. 2026; 360: 151856.
[44] Jayaraman S, Eswaran A, Rajagopal P, Palanisamy CP, Veerakumar P, Veeraraghavan VP, Sirasanagandla SR. Neuroendocrine-associated epigenetic factors in cellular senescence: mechanisms and therapeutic implications. Biogerontology. 2026; 27(2): 64.
[45] Ponnusamy B, Rajagopal P, Palanisamy CP, Veeraraghavan VP, Jayaraman S. Mechanistic Exploration of the anticancer activity of Justicia adhatoda Plant Leaf Ethanolic Extract against Colon Cancer Cells: An in silico and in vitro Approach. Asian Pacific Journal of Cancer Prevention. 2026; 27(3): 1069-1080.
[46] Pei J, Saran VS, Sivaramakrishnan R, Kanniappan GV, Pandurangan V, Jayaraman S, Dhayalan VK, Mironescu M, Mironescu ID, Palanisamy CP. Ultrasonic-assisted, Sargassum ilicifolium (brown marine macroalgae)-mediated biogenic synthesis of CuO nanoparticles incorporated in starch/PVA electrospun nanoscaffolds: In vitro safety and antioxidant efficacy assessment. Bioorganic Chemistry. 2026; 173: 109679.
[47] Raj MAPA, Subramaniyam S, Kanniappan GV, Jayaraman S, Palanisamy CP. Sustainable fabrication of starch/PVA/CuO electrospun nanoscaffolds from Turbinaria ornata (marine macroalgae) extract: Physicochemical characterization and antidiabetic evaluation. Kuwait Journal of Science. 2026; 53(2): 100545.
[48] Pei J, Ganesh NS, Subramaniyam S, Sivaramakrishnan R, Kanniappan GV, Jayaraman S, Palanisamy CP. Sustainable fabrication of starch/PVA/CuO electrospun nanoscaffolds from Padina tetrastromatica (Brown macroalgae) extract: Physicochemical characterization and antidiabetic assessment. Sustainable Chemistry One World. 2026; 9: 100195.

[49] Sakthiraj A, Sivaramakrishnan R, Subramaniyam S, Kanniappan GV, Pandurangan V, Jayaraman S, Dhayalan VK, Mironescu M, Mironescu ID, Palanisamy CP. Starch/PVA electrospun nanoscaffolds loaded with ultrasonic-assisted green-synthesis of CuO nanoparticles from marine macroalgae (Gracilaria corticata) extract: Cytotoxicity and antioxidant analysis. Chemical Physics Impact. 2026; 12: 101018.
[50] Raju M, Chandrasekaran MK, Loganathan L, Ahalliya RM, Mironescu M, Mironescu ID, Palanisamy CP, Kanniappan GV. Lipid remodeling and ferroptosis in phosphatidylcholine-mediated tumor–stroma crosstalk. Frontiers in Molecular Biosciences. 2026; 13: 1742305.
[51] Kunamalla R, Panagal M, Palanisamy CP. Biogenic synthesis and fabrication of starch/PVA/CuO electrospun nanoscaffolds from Sargassum ilicifolium (brown marine macroalgae) extract for anticancer activity on HT-29 and MCF-7 cancer cells. Biocatalysis and Agricultural Biotechnology. 2026; 72: 103923.
[52] Pei J, Govindaraj H, Sivaramakrishnan R, Kanniappan GV, Pandurangan V, Dhayalan VK, Mironescu M, Mironescu ID, Jayaraman S, Palanisamy PC. Sustainable fabrication of biopolymer-based (starch/PVA) nanoscaffolds loaded with green-synthesized CuO nanoparticles from Sargassum wightii (marine macroalgae): Cytocompatibility and antioxidant activity. Biomaterials Advances. 2026; 182: 214660.
[53] Pei J, Perumal NC, Meng P, Long Q, Palanisamy CP. Extracellular vesicle-based biosensors for Alzheimer's disease: A new frontier in precision diagnostics. Ageing Research Reviews. 2026; 113: 102904.
[54] Shree P, Sivaramakrishnan R, Kanniappan GV, Pandurangan V, Jayaraman S, Dhayalan VK, Mironescu M, Mironescu ID, Palanisamy CP. Antioxidant and biocompatible CuO-starch/PVA nanoscaffolds via ultrasonic green synthesis using Turbinaria conoides (brown marine macroalgae). Medicine in Drug Discovery. 2025; 28: 100238.
[55] Gong J, Lin J, Guan T, Pei J, Palanisamy CP, El-AtyFrom AMA. selenium tolerance to nanoplastic antagonism: Comprehensive characterization of L. casei SNUT1 and its extracellular vesicle–nanoselenium complex. Food Bioscience. 2025; 74: 107749.
[56] Poochi SP, Sundarraj R, Raju MV, Chandrasekaran MK, Ahalliya RM, Palanisamy CP, Kanniappan GV, Kondapavuluri BK, Thiruvengadam M. Harnessing Nature: Computational and Experimental Insights Into *Ipomoea obscura* Metabolites for Bladder Cancer Therapy. Chemistry and Biodiversity. 2025; 0: e00909.
[57] Dugganaboyana GK, Kannankumar MKG, Shivaramakrishna S, Raju MV, Chandrasekaran MK, Ahalliya RM, Panneerselvam N, Palanisamy CP, Kanniappan GV. Phytochemical insights, antioxidant activity and therapeutic potential of Cassia senna against prostate cancer in Wistar albino rats. Discover Applied Sciences. 2025; 7:1206.
[58] Natarajan SR, Krishnamoorthy R, Alshuniaber MA, Gatasheh MK, Rajagopal P, Veeraraghavan VP, Palanisamy CP, Jayaraman S. KDM1A Facilitates Oncogenic Potential in Colorectal Cancer Progression Through the Activation of AXIN/GSK3β/β-Catenin Signaling Pathways: Evidence From Integrated Transcriptomics and In Vitro Studies. The Journal of Gene Medicine. 2025; 27(11): e70053.
[59] Natarajan PM, Umapathy VR, Murali A, Swamikannu B. (2022). Computational Simulations of Identified marine-derived Natural Bioactive Compounds As Potential Inhibitors of Oral Cancer. Future Science OA. 2022; 8(3).
[60] Natarajan PM, Umapathy VR. Role of transcriptomics in the study of oral cancer. Frontiers in Oral Health. 2025; 6:1524364.
[61] Vidhyarekha U, Natarajan PM, Bhuminathan S, Sabarinathan J, Suba R, Vijayalakshmi P. Role of artificial intelligence in Oral Cancer. Advances in Public Health. 2024. 2024: 3664408.
[62] Ganesan A, Kumar NG, Natarajan PM, Gauthaman J. Automated classification of elongated styloid processes using deep learning models-an artificial intelligence diagnostics. Frontiers in Oral Health. 2025; 5: 1424840.
[63] Umapathy VR, Natarajan PM, Swamikannu B. Regenerative Strategies in Dentistry: Harnessing Stem Cells, Biomaterials and Bioactive Materials for Tissue Repair. Biomolecules. 2025; 15: 546.
[64] Natarajan PM. Dental Bioinformnatics-Current Scope and Future perspectives. Research Journal of Pharmacy and Technology. 2022;15(5):2351-6.
[65] Xi J, Wang T, Xian P, Liu X, Du M, Yang H, Palanisamy CP, Lin W, Long Q. Proteomic insights uncover enhanced neurotherapeutic potential in conditioned mesenchymal stem cell-derived extracellular vesicles. Extracellular Vesicle. 2024; 3: 100037.
[66] Pei J, Natarajan PM, Umapathy VR, Swamikannu B, Sivaraman NM, Krishnasamy L, Palanisamy CP. Advancements in the synthesis and functionalization of zinc oxide-based nanomaterials for enhanced oral cancer therapy. Molecules. 2024; 29(11): 2706.
[67] Gatasheh MK, Natarajan SR, Krishnamoorthy R, Alsulami TS, Rajagopal P, Palanisamy CP, Veeraraghavan VP, Jayaraman S. Molecular analysis to identify novel potential biomarkers as drug targets in colorectal cancer therapy: an integrated bioinformatics analysis. Molecular and Cellular Oncology. 2024; 11(1): 2326699.
[68] Pei J, Yan Y, Jayaraman S, Rajagopal P, Natarajan PM, Umapathy VR, Gopathy S, Roy JR, Sadagopan CS, Thalamati D, Palanisamy CP, Mironescu M. A review on advancements in the application of starch-based nanomaterials in biomedicine: Precision drug delivery and cancer therapy. International Journal of Biological Macromolecules. 2024; 130746.

[69] Pei JJ, Yan Y, Palanisamy CP, Jayaraman S, Natarajan PM, Umapathy VR, Gopathy S, Roy JR, Sadagopan JC, Thalamati D, Mironescu M. Materials-based drug delivery approaches: Recent advances and future perspectives. Green Processing and Synthesis. 2024; 13: 20230094.
[70] Pei JJ, Deng W, Liu Y, Guo Y, Chen J, Abdu H, Khan MR, Palanisamy CP, El-Aty AM. A Comprehensive Review of Cornus officinalis: Health Benefits, Phytochemistry, and Pharmacological Effects for Functional Drug and Food Development. Frontiers in Nutrition. 2023; 10: 1309963.
[71] Alugoju P, Palanisamy CP, Anthikapalli NVA, Jayaraman S, Prasanskulab A, Chuchawankul S, Dyavaiah M, Tencomnao T. Exploring the anti-aging potential of natural products and plant extracts in budding yeast Saccharomyces cerevisiae: A review. F1000Research. 2023; 12: 1265.
[72] Lavanya M, Krishnamoorthy R, Alshuniaber MA, Manoharadas S, Palanisamy CP, Veeraraghavan VP, Jayaraman S, Rajagopal P, Padmini R. Formulation, characterization and evaluation of gelatin-syringic acid/zinc oxide nanocomposite for its effective anticancer, antioxidant and anti-inflammatory activities. Journal of King Saud University-Science. 2023; 35: 102909.
[73] Palanisamy CP, Poompradub S, Sansanaphongpricha K, Jayaraman S, Subramani K, Sonsudin F. Biosynthesis of silver nanoparticles (AgNPs) using ethanolic extract of Nigella sativa (L.) seeds promotes wound healing via PDGF and VEGF signalling pathways activation. Biocatalysis and Agricultural Biotechnology. 2023; 54: 102970.
[74] Prasad M, Jayaraman S, Natarajan SR, Veeraraghavan VP, Krishnamoorthy R, Gatasheh MK, Palanisamy CP, Elrobh M. Piperine modulates IR/Akt/GLUT4 pathways to mitigate insulin resistance: Evidence from animal and computational studies. International Journal of Biological Macromolecules. 2023; 253: 127242.
[75] Palanisamy CP, Pei JJ, Phaniendra A, Venkata AAN, Jayaraman S, Veeraragahavan VP, Sridevi G, Roy JR, Janaki CS, Thalamati D, Mironescu M, Luo Q, Chai Y, Long Q. New Strategy of Neurodegenerative Disease Treatment with Extracellular Vesicles (EVs) Derived from Mesenchymal Stem Cells (MSCs). *Theranostics*. 2023; 13(12):4138-4165. doi:10.7150/thno.83066.
[76] Palanisamy CP, Phaniendra A, Jayaraman S, Poompradub S. *Nigella sativa* L. seed extracts promotes wound healing progress by activating VEGF and PDGF signalling pathways: *An in vitro* and *in silico* study. *F1000 Research*. 2023; 12: 436.
[77] Pei JJ, Palanisamy CP, Phaniendra A, Venkata AAN, Natarajan PM, Umapathy VR, Swamikannu B, Jayaraman S, Rajagopal P, Poompradub S. A comprehensive review on bio-based materials for chronic diabetic wounds. *Molecules*. 2022; 28(2), 604.
[78] Palanisamy CP, Cui B, Zhang H, Gunasekaran VP, Ariyo A, Jayaraman S, Veeraraghavan V, Rajagopal P. A critical review on starch-based electrospun nanofibrous scaffolds for wound healing application. International Journal of Biological Macromolecules. 2022; 222 (Part: B): 1852-1860.